Available online at www.sciencedirect.com
ScienceDirect
Precision Engineering 32 (2008) 63–70
PRECISION ENGINEERING
www.elsevier.com/locate/precision

Review

Review of circular flexure hinge design equations and derivation of empirical formulations

Yuen Kuan Yong *, Tien-Fu Lu, Daniel C. Handley

School of Mechanical Engineering, The University of Adelaide, SA 5005, Australia

Received 6 February 2006; accepted 16 May 2007
Available online 14 July 2007

Abstract

This article presents the comparison of various compliance/stiffness equations of circular flexure hinges with FEA results. The limitation of these equations at different t/R (R is the radius and t is the neck thickness) ratios are revealed. Based on the limitations of these design equations, a guideline for selecting the most accurate equations for hinge design calculations are presented. In addition to the review and comparisons, general empirical stiffness equations in the x- and y-direction were formulated in this study (with errors less than 3% when compared to FEA results) for a wide range of t/R ratios ($0.05 \leq t/R \leq 0.8$).

Keywords: Circular flexure hinges; Empirical hinge design equations; Finite element analysis

Contents

* Corresponding author. Tel.: +61 249216438; fax: +61 249216993.
E-mail address: Yuenkuan.Yong@newcastle.edu.au (Y.K. Yong).

0141-6359/$ – see front matter.
doi:10.1016/j.precisioneng.2007.05.002

1. Introduction

Flexure hinges have been widely used in applications such as gyroscopes, accelerometers, balance scales, missile-control nozzles and multiplying linkages [1]. Furthermore, micromanipulation has emerged as an important technological advancement in the past decade that increases the use of flexure hinges. Micro-manufacturing, micro-system assembly, biological cell manipulation in biotechnology and MEMS (micro-electromechanical system) increase the demand of ultra-precision manipulation stages which are used to manipulate micro-scale objects and perform very small motions (less than 100 μm). Various micro-motion stages were developed using conventional technologies based on servomotors, ball screws and rigid linkages. However, these conventional technologies encounter problems such as friction, wear, backlash and lubrication, which struggle to achieve high positioning accuracy. On the other hand, compliant micro-motion stages, which solely move through deformations of flexure hinges, provide smooth motions without encountering problems aforementioned. Therefore, compliant stages with flexure hinges are capable of achieving highly precise positioning [2].

Despite all the advantages aforementioned, there are some disadvantages associated with compliant micro-motion stages with flexure hinges. For example, it is more complicated to model and to control the motions of compliant stages precisely compared to conventional mechanisms. This could be partly attributed to parasitic motions of flexure hinges in the x- and y-direction. The commonly adopted compliant micro-motion stage modeling method, named the pseudo-rigid-body model (PRBM), models a flexure hinge in a compliant stage as a revolute joint (connecting two links) with a torsional spring attached to it. The PRBM does not model parasitic motions of flexure hinges mathematically; these parasitic motions do cause noticeable position errors between analytical and experimental results [3].

A precise compliant stage model will benefit researchers in, at least, the design and optimization phases where a good estimation of workspace or stiffness of a micro-motion stage could be realized. A compliant micro-motion stage normally uses a few flexure hinges to provide the desired motions of the stage in various directions. The accuracy of a compliant stage model relies on the precision of flexure hinge modeling. Therefore, compliance/stiffness equations of flexure hinges are demanded to be as accurate as possible to reduce the accumulated modeling errors of hinges, thus reducing the overall modeling errors of compliant stages.

Due to the importance of precise compliance/stiffness equations of flexure hinges aforementioned, this article presents a review on the accuracies of various compliance/stiffness equations of flexure hinges derived using different methods. This review could served as a guideline for designers to selecting the most suitable and accurate compliance/stiffness equations for precise hinge and compliant stage design calculations. Circular flexure hinges were chosen to be studied due to its large applications in compliant micro-motion stages [2–7] which required high precision of motions. Circular flexure hinges are precise in rotation where their center of rotations do not displace as much as other flexure hinges such as the left-type [8] and the corner-fillet [9]. There have been many methods adopted to derive satisfactory compliance/stiffness equations of flexure hinges, including the integration of linear differential equations of a beam [1,10,11], Castigliano's second theorem [11], inverse conformal mapping [8] and empirical equations formed from FEA (finite element analysis) results [12,13]. However, some of these methods provide better accuracies than the others depending on the t/R ratios of circular flexure hinges (see Fig. 1 for dimensions). Paros and Weisbord [1] were the first research group to introduce right circular flexure hinges. They formulated design equations, including both the full and simplified, to calculate compliances of flexure hinges. The error of the simplified equation relative to full equation was within 1% for hinges with t/R in the range 0.02–0.1, and within 5–12% for thicker hinge with t/R in the range 0.2–0.6 [8]. However, both the full and simplified rotational compliance equations (α_z/M_z) show a large difference of up to 25% or more for $t/R = 0.6$ when compared with FEA results [8].

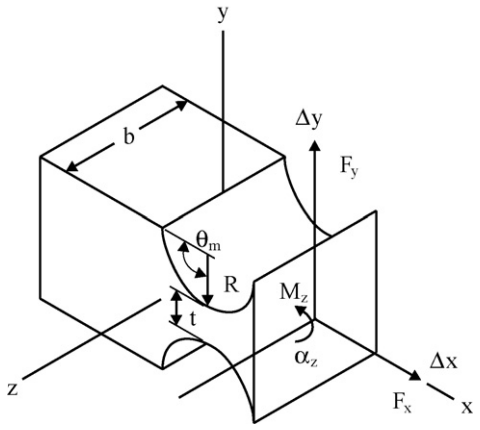

Fig. 1. Flexure hinge.

A comparison of Smith's experimental results [14](M_z/α_z) with Paros and Weisbord's results was conducted in this study. The comparison revealed that the simplified equation shows a difference of up to 10% and the full equation shows a difference of up to 16%. It was also found by Smith et al. that Paros and Weisbord's full equation of α_z/M_z had larger errors than the simplified equation when compared with the FEA results [14]. Wu and Zhou developed concise compliance equations based on Paros and Weisbord's full equations [10]. Their design equations have the same results as that of Paros and Weisbord's full equation, except signs of α_z/F_z and $\Delta y/M_z$ were opposite. Therefore, Wu and Zhou's results have the same percentage errors as Paros and Weisbord's results (neglecting signs) aforementioned. Tseytlin developed rotational compliance equations (α_z/M_z) for circular and elliptical flexure hinges using the inverse conformal mapping method [8]. Tseytlin categorized hinges into three groups, named thin ($t/R \leq 0.07$), intermediate ($0.07 < t/R \leq 0.2$) and thick ($0.2 < t/R \leq 0.6$), and an equation was derived to calculate compliances for each category respectively. He claimed that the conformal mapping equations

were within 10% error when comparing with FEA and experimental results. Smith et al. derived an empirical equation from FEA results to calculate rotational compliances [12]. This equation is tractable and adequate only for thick hinges with t/R in the range 0.2–1.0 [8]. Lobontiu et al. derived closed form compliance equations using Castigliano's second theorem [15]. The analytical compliance results for hinges, with t/R equal to 0.05, 0.1 and 0.2, were compared with FEA results and the percentage errors were within 10%. There is no comparison of results presented for other t/R ratios.

There are various compliance/stiffness equations available for design calculations of circular flexure hinges. Comparisons among analytical, FEA and experimental results were conducted by some researchers only for α_z/M_z and were limited to certain t/R range. There is no proper scheme to guide designers for selecting the most accurate design equations out of all the previously mentioned methods which could precisely calculate compliance/stiffness of flexure hinges for a wide t/R range. Thus, this article presents a review on the limitations of various compliance/stiffness equations (derived using different methods) of circular flexure hinges, at different t/R ratios, based on their percentage errors when compared to FEA results. By analyzing the limitations of each design equation, suggestions of the most accurate and appropriate equations to be used at any particular t/R range are provided in this article. In addition to the review and comparisons, general empirical equations were developed based on FEA results to estimate compliance/stiffness in the x- and y-axis as there is no accurate equation (within 5%) to predict the corresponding compliance/stiffness of circular flexure hinges for a wide t/R range ($0.05 \leq t/R \leq 0.8$).

2. FEA modeling of circular flexure hinges

Due to the limitation of available experimental results, (only three experimental results were found from Smith et al. [14], for three t/R cases) FEA results in this article were used as a benchmark for comparison of various compliance/stiffness results for a wide range of t/R. The accuracies of these FEA models were within 3% error when compared with the three experimental results of Smith et al. [14].

ANSYS was used to conduct FEA of flexure hinges. Flexure hinge models were generated using 8-node, two-dimensional, plane elements (PLANE82) with two degree-of-freedom on each node, which are translations in the nodal x- and y-directions. This element type is more suitable to model irregular shapes and curved boundaries without much loss of accuracy [16]. The modeled flexure hinges had a thickness of 12.7 mm (aluminium alloy, 7075-T6) with a Young's modulus (E) of 71.7 GPa and a Poisson ratio (ν) of 0.33. A mapped meshing technique was used instead of a "smart" meshing, the later automatically produces fine meshing at areas that high stress concentrations were most likely to occur. Mapped meshing is advantageous over "smart" meshing because mapped meshing provides better control of the distribution and size of elements in an area (see Fig. 2). It was found that the accuracy of the FEA model was significantly influenced by the way the boundary conditions were assigned on a model. For example, when a point force is applied on a node,

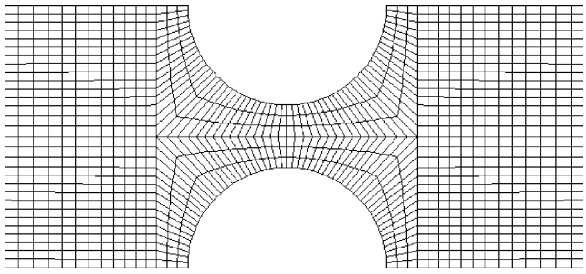

Fig. 2. FEA mapped meshing.

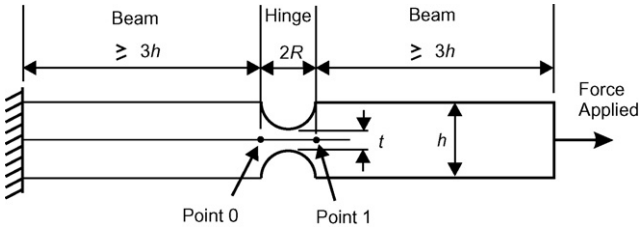

Fig. 3. Flexure hinge geometries of a FEA model.

it could cause a local stress spike on the node which reduces the accuracy of the FEA results. Therefore, constraints and forces were applied at a distance of at least $3h$ (see Fig. 3) from a node where its displacements will be read, to reduce influences of the constraints and applied forces on the FEA results. Forces in the x- and y-direction and a moment along the z-direction were applied. The corresponding nodal deformations at point 0 and point 1 were read. This ANSYS modeling technique is similar to that of Lobontiu et al.'s [15,17]. Analytical design equations [1,8,10–12] were derived to calculate compliances at point 1. However, nodal deformations read from FEA results at point 1 were the total deformation contributed by the left-hand side beam section as well as the hinge section (see Fig. 3). Therefore, rotations and deformations caused by the beam section (nodal deformations at point 0) were subtracted from total deformations read at point 1 to obtain pure deformations caused by the hinge.

3. Comparison of compliance/stiffness results with FEA

3.1. Rotational compliance equations, α_z/M_z

Compliances, α_z/M_z of different right circular flexure hinges (with various t and R values), where t/R in a range 0.05–0.65, were calculated using design equations of (a) Paros and Weisbord [1] (full), (b) Paros and Weisbord [1] (simplified), (c) Lobontiu [11], (d) Wu and Zhou [10], (e) Tseytlin [8], (f) Smith et al. [12] (empirical) and (g) Schotborgh et al. [13] (empirical). Their results were compared with the FEA results obtained in this article. Percentage errors of the comparisons were plotted in Fig. 4. Those design equations are presented in Appendix A. From Fig. 4, it was noted that

- Equations of Paros and Weisbord (full), Lobontiu and Wu and Zhou were derived using a similar method (that is the integration of the linear differential equation of a beam); thus

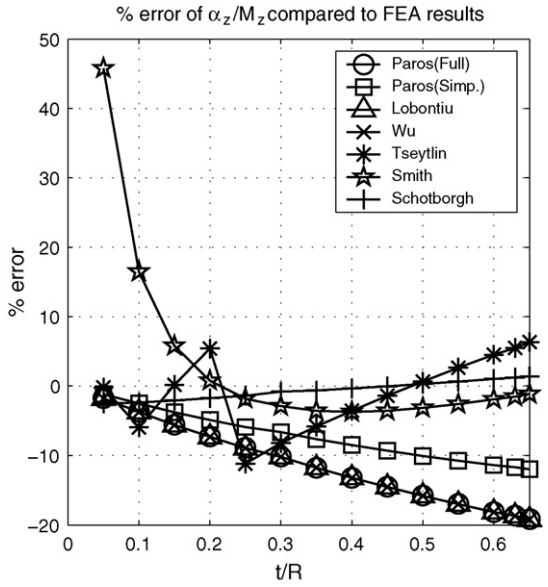

Fig. 4. Percentage errors of α_z/M_z compared to FEA results.

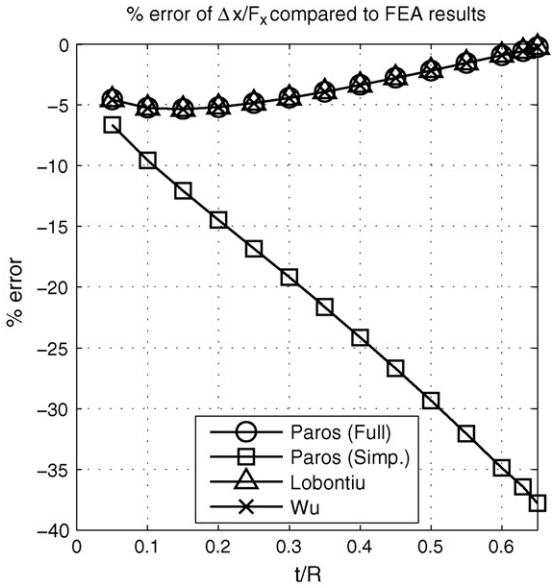

Fig. 5. Percentage errors of $\Delta x/F_x$ compared to FEA results.

they have the same percentage errors when compared with FEA results. The accuracies of their results decrease over the t/R range. Errors are less than 5% when $0.05 \leq t/R < 0.15$. Errors increase to more than 5% but less than 10% when $0.15 \leq t/R < 0.3$. When $0.3 \leq t/R \leq 0.65$, errors increase from 10% to 19.2%.

- Paros and Weisbord's (simplified) results are accurate within 5% error for $0.05 \leq t/R \leq 0.2$. Errors increase up to 10% when $t/R = 0.5$ and 12% when $t/R = 0.65$.
- Tseytlin's results are accurate (within 6% error) for $t/R \leq 0.23$ and $0.35 \leq t/R < 0.65$. Errors increase to more than 6% when $0.23 < t/R < 0.35$. When $t/R = 0.25$, the error is 11.2%. Generally, the results are within 10% error approximately for the entire t/R range. Interestingly, Tseytlin's analytical results differed from his experimental and FEA results by about 10% [8]. This suggests the accuracy of FEA results in this article match the accuracy of Tseytlin's analytical and FEA results.
- Smith et al.'s (empirical) rotational compliance equation is only accurate (within 4% error) for $0.20 \leq t/R \leq 0.65$. This observation is similar to that of Tseytlin where he claimed that Smith et al.'s empirical equation is accurate only for thick flexure hinges with t/R in the range 0.2–1.0.
- Schotborgh et al.'s results are the most accurate compared to the rest. Errors in their results are less than 2.5% for the whole $0.05 \leq t/R \leq 0.65$ range.

3.2. Compliance equations in the x- and y-direction, $\Delta x/F_x$ and $\Delta y/F_y$

Percentage errors of $\Delta x/F_x$ and $\Delta y/F_y$, calculated using design equations of (a) Paros and Weisbord [1] (full), (b) Paros and Weisbord [1] (simplified), (c) Lobontiu [11] and (d) Wu and Zhou [10] were plotted in Figs. 5 and 6 respectively.

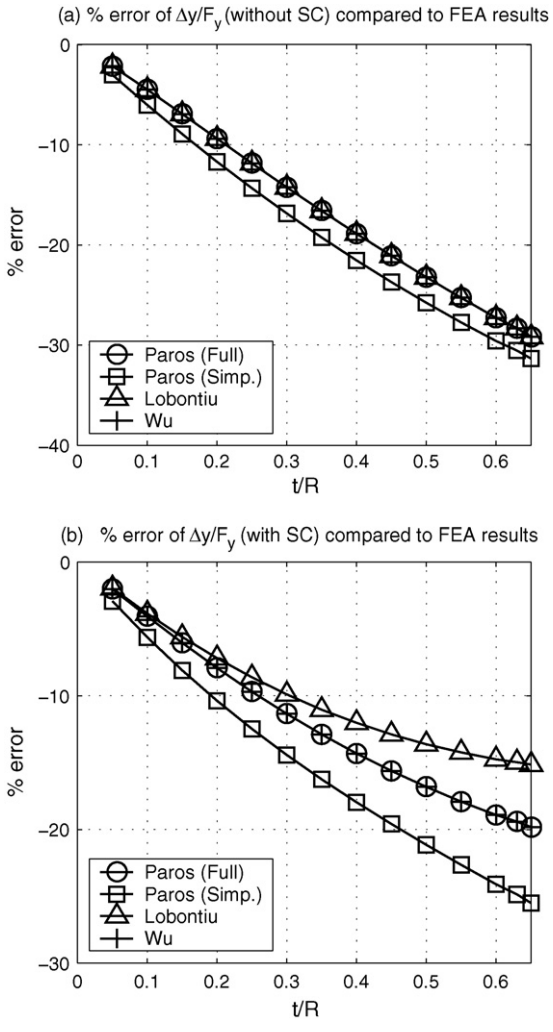

Fig. 6. Percentage errors of $\Delta y/F_y$ compared to FEA results. (a) Without shear compliance and (b) with shear compliance.

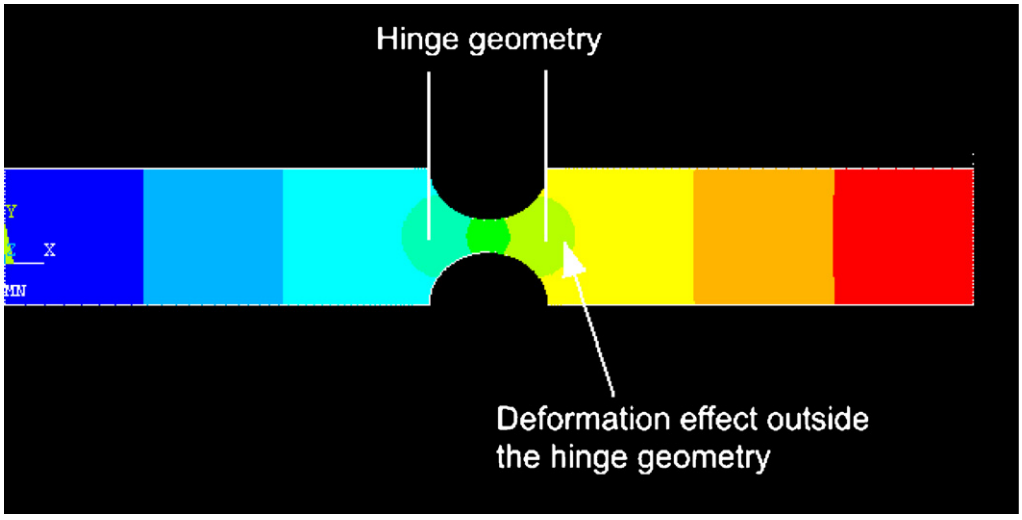

Fig. 7. Deformation effect outside flexure hinge geometry (figure was provided by Schotborgh).

For $\Delta x/F_x$,

- Paros and Weisbord (full), Lobontiu, and Wu and Zhou have the same results. Their results are within 6% error compared to FEA results.
- Results of Paros and Weisbord (simplified) are not as accurate as that of Paros and Weisbord (full), Lobontiu, and Wu and Zhou. Their results have a minimum error of 6.6% and a maximum error of 38%.

For $\Delta y/F_y$ (without shear compliance, SC),

- Results of Paros and Weisbord (full), Lobontiu, and Wu and Zhou, without considering shear compliance (SC), are the same. Their percentage errors are within 10% for $0.05 \leq t/R \leq 0.2$. Errors increase up to 30% when $t/R = 0.65$.
- Paros and Weisbord's (simplified) results are within 10% when $0.05 \leq t/R \leq 0.17$. Errors increase to 31% when $t/R = 0.65$.

For $\Delta y/F_y$ (with shear compliance, SC),

- Lobontiu's results are the most accurate compared to the others. The results are within 5% error for $0.05 \leq t/R \leq 0.1$. The errors increase to within 10% for $0.1 < t/R \leq 0.3$ and to within 15% for $0.3 < t/R \leq 0.65$.
- Results of Paros and Weisbord's (full) and Wu and Zhou are the same. Their results are within 5% error for $0.05 \leq t/R \leq 0.1$. The errors increase to within 10% for $0.1 < t/R \leq 0.25$ and to within 20% for $0.25 < t/R \leq 0.65$.
- Paros and Weisbord's (simplified) results are within 5% error for $0.05 \leq t/R < 0.1$. The errors increase to within 10% for $0.1 \leq t/R \leq 0.17$. The maximum error is 25.5% when $t/R = 0.65$.

Generally, all compliance equations, $\Delta y/F_y$ are more accurate when shear compliances are considered. Schotborgh's empirical stiffness/compliance equations in the x- and y-direction were not compared in this article because his equations were derived using hinge models with different height (h, see Fig. 3). Furthermore, his empirical equations consider the deformation effect outside the hinge geometry (as told via a personal communication with Schotborgh). From Fig. 7, it can be seen that the deformation effect of the hinge goes beyond the hinge geometry to the beam section. Other research groups (which are [1,11,10]) did not consider this effect in their equations. The aspect of this deformation effect on the hinge compliances is beyond the scope of this paper. The significance of this effect are currently being investigated and will be revealed in near future.

4. Empirical compliance/stiffness equations in the x- and y-direction

From previous section, it was noted that there is no accurate design equations (within 5% error) at this stage to estimate compliances/stiffness in the y-direction for $t/R > 0.15$ and in the x-direction for $0.1 < t/R < 0.25$. Therefore, general empirical equations (in stiffness form, named K_x and K_y) were formed based on FEA results to estimate stiffness in both the x- and y-direction for a wide range of t/R ratios ($0.05 \leq t/R \leq 0.8$). FEA models with various t/R ratios, which was set from 0.05 to 0.8 with increment of 0.01, were generated in ANSYS. Unit forces, F_x and F_y were applied on each model and the corresponding deformations, Δx and Δy were read. Polynomial functions

Table 1
Coefficients of polynomial functions for K_x and K_y

Coefficients	K_x (fifth order)	K_y (sixth order)
c_0	0.036343	1.92×10^{-5}
c_1	0.98683	−0.00083463
c_2	−1.5469	0.021734
c_3	3.1152	0.064783
c_4	−3.0831	−0.088075
c_5	1.2031	0.062278
c_6	–	−0.018781

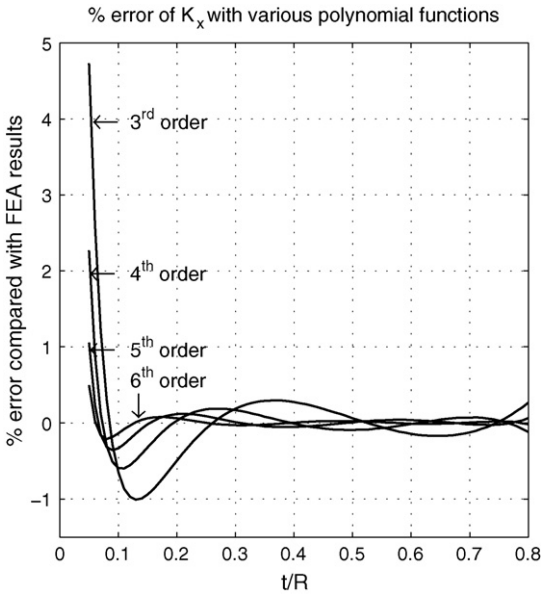

Fig. 8. Percentage errors of empirical equations, K_x.

with third, fourth, fifth and sixth order were fitted through the data points to obtain empirical stiffness equations. The results of these four empirical equations were compared with FEA results and the percentage errors were plotted in Figs. 8 and 9. Fifth and sixth order polynomial functions were used for K_x and K_y, respectively in order to keep the errors as small as possible. By using the two polynomial functions, maximum errors occurred when $t/R = 0.05$, which are 1.1% and 2.7% for K_x and K_y, respectively. Both empirical equations are shown in Eqs. (1) and (2). Table 1 exhibits coefficients of these equations

$$K_x = Eb\left[\sum_{k=0}^{n} c_k \left(\frac{t}{R}\right)^k\right] \tag{1}$$

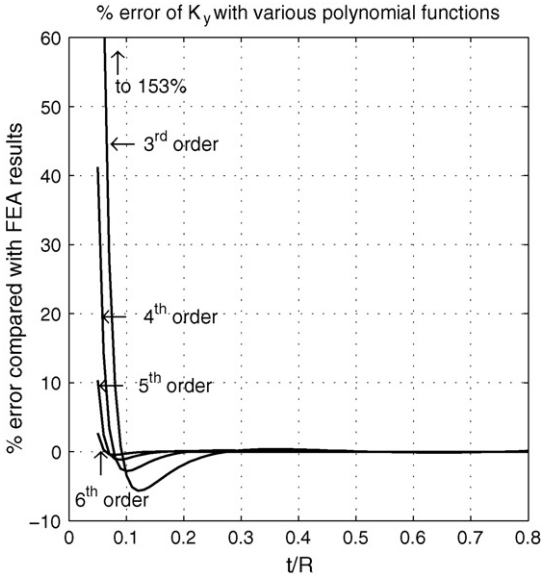

Fig. 9. Percentage errors of empirical equations, K_y.

Table 2
Suggested compliance/stiffness equations for a particular t/R range

Research group	α_z/M_z (t/R range)	% error			$\Delta y/F_y$ (with SC) (t/R range)	% error			$\Delta x/F_x$ (t/R range)	% error		
		Minimum	Maximum	Average		Minimum	Maximum	Average		Minimum	Maximum	Average
PW[a](full)	$0.05 \le t/R < 0.1$	1.8	5.0	3.5	$0.05 \le t/R \le 0.1$	2	4	3.1	$0.25 \le t/R \le 0.65$	0.3	4.9	2.4
PW[a](simpl.)	$0.05 \le t/R \le 0.2$	1.2	4.9	3.1	$0.05 \le t/R \le 0.1$	3	5.6	4.3		Not recommended		
Lobontiu	$0.05 \le t/R < 0.1$	1.8	5.0	3.5	$0.05 \le t/R \le 0.1$	2	3.9	2.9	$0.25 \le t/R \le 0.65$	0.3	4.9	2.4
Wu and Zhou	$0.05 \le t/R < 0.1$	1.8	5.0	3.5	$0.05 \le t/R \le 0.1$	2	4	3.1	$0.25 \le t/R \le 0.65$	0.3	4.9	2.4
Tseytlin	$0.4 \le t/R \le 0.6$	0.7	4.5	2.5	NA	NA	NA	NA	NA	NA	NA	NA
Smith	$0.2 \le t/R \le 0.65$	0.8	3.7	2.4	NA	NA	NA	NA	NA	NA	NA	NA
Schotborgh	$0.05 \le t/R \le 0.65$	0.03	2.5	1.2	NA	NA	NA	NA	NA	NA	NA	NA
This article	NA	NA	NA	NA	$0.05 \le t/R \le 0.8$	0	2.7	0.07	$0.05 \le t/R \le 0.8$	0	1.1	0.08

[a] Paros and Weisbord.

$$K_y = Eb\left[\sum_{k=0}^{n} c_k \left(\frac{t}{R}\right)^k\right] \tag{2}$$

where c_k are coefficients of polynomial functions and n is the order of a polynomial function.

Finally, Table 2 summarizes the suggested compliance/stiffness equations to be used for any particular t/R range, and their minimum, maximum and average percentage errors.

5. Conclusions

This article presents a review on the accuracies of various circular flexure hinge equations by comparing the results of design equations to that of FEA. Based on the results of comparisons, a guideline for selecting the most suitable and accurate compliance/stiffness equations for hinge design calculations is presented. In addition to the review and comparisons, general empirical stiffness equations in the x- and y-direction, other than the bending direction, were formulated in this study for a wide range of t/R ratios ($0.05 \le t/R \le 0.8$). The percentage errors of these empirical equations were found to be less than 3% when compared to FEA results.

Acknowledgements

The authors would like to greatly acknowledge the support of the Adelaide Robotics Research Group at the University of Adelaide and the use of its facilities. Also, a special thanks to Dr. Andrei Kotousov and Dr. Carl Howard for their great advices on FEA modelling and their valuable time.

Appendix A. Circular flexure hinge design equations

A.1. Paros and Weisbord [1]

A.1.1. Full equations

$\beta = t/2R$, $\gamma = 1 + \beta$, $\theta_m = \pi/2$ for right circular flexure hinge

$$\frac{\alpha_z}{M_z} = \frac{3}{2EbR^2}\left[\frac{1}{2\beta+\beta^2}\right]\left\{\left[\frac{1+\beta}{\gamma^2} + \frac{3+2\beta+\beta^2}{\gamma(2\beta+\beta^2)}\right] \times \left[\sqrt{1-(1+\beta-\gamma)^2}\right] + \left[\frac{6(1+\beta)}{(2\beta+\beta^2)^{3/2}}\right] \times \left[\tan^{-1}\left(\sqrt{\frac{2+\beta}{\beta}} \times \frac{(\gamma-\beta)}{\sqrt{1-(1+\beta-\gamma)^2}}\right)\right]\right\} \tag{A.1}$$

$$\frac{\Delta y}{F_y} = R^2 \sin^2\theta_m \left(\frac{\alpha_z}{M_z}\right) - \frac{3}{2Eb}\left\{\left[\frac{1+\beta}{(1+\beta-\cos\theta_m)^2} - \frac{2+(1+\beta)^2/(2\beta+\beta^2)}{(1+\beta-\cos\theta_m)}\right] \times \sin\theta_m + \left[\frac{4(1+\beta)}{\sqrt{2\beta+\beta^2}} - \frac{2(1+\beta)}{(2\beta+\beta^2)^{3/2}}\right] \times \tan^{-1}\sqrt{\frac{2+\beta}{\beta}}\tan\frac{\theta_m}{2} - (2\theta_m)\right\} \tag{A.2}$$

$$\frac{\Delta x}{F_x} = \frac{1}{Eb}\left[-2\tan^{-1}\frac{\gamma-\beta}{\sqrt{1-(1+\beta-\gamma)^2}} + \frac{2(1+\beta)}{\sqrt{2\beta+\beta^2}}\tan^{-1}\left(\sqrt{\frac{2+\beta}{\beta}} \times \frac{\gamma-\beta}{\sqrt{1-(1+\beta-\gamma)^2}}\right)\right] \tag{A.3}$$

Shear compliance: shear modulus, $G = E/[2(1+\nu)]$

$$\left[\frac{\Delta y}{F_y}\right]_s = \frac{1}{Gb}\left[-\theta_m + \frac{2(1+\beta)}{\sqrt{2\beta+\beta^2}} \times \tan^{-1}\sqrt{\frac{2+\beta}{\beta}}\tan\frac{\theta_m}{2}\right] \tag{A.4}$$

A.1.2. Simplified equations

$$\frac{\alpha_z}{M_z} = \frac{9\pi R^{1/2}}{2Ebt^{5/2}} \tag{A.5}$$

$$\frac{\Delta y}{F_y} = \frac{9\pi}{2Eb}\left(\frac{R}{t}\right)^{5/2} \tag{A.6}$$

$$\frac{\Delta x}{F_x} = \frac{1}{Eb}[\pi(R/t)^{1/2} - 2.57] \tag{A.7}$$

Shear compliance: shear modulus, $G = E/[2(1+\nu)]$

$$\left[\frac{\Delta y}{F_y}\right]_s = \frac{1}{Gb}[\pi(R/t)^{1/2} - 2.57] \tag{A.8}$$

A.2. Lobontiu [11]

$$\frac{\alpha_z}{M_z} = \frac{24R}{Ebt^3(2R+t)(4R+t)^3}\left[t(4R+t)(6R^2+4Rt+t^2) + 6R(2R+t)^2\sqrt{t(4R+t)}\arctan\left(\sqrt{1+\frac{4R}{t}}\right)\right] \tag{A.9}$$

$$\frac{\Delta y}{F_y} = \frac{3}{4Eb(2R+t)}\left\{2(2+\pi)R + \pi t + \frac{8R^3(44R^2+28Rt+5t^2)}{t^2(4R+t)^2} + \frac{(2R+t)\sqrt{t(4R+t)}}{\sqrt{t^5(4R+t)^5}} \times \left[-80R^4 + 24R^3t + 8(3+2\pi)R^2t^2\right.\right.$$

$$+4(1+2\pi)Rt^3+\pi t^4\Big] - \frac{8(2R+t)^4(-6R^2+4Rt+t^2)}{\sqrt{t^5(4R+t)^5}} \times \left(\arctan\sqrt{1+\frac{4R}{t}}\right)\Bigg\} \quad (A.10)$$

$$\frac{\Delta x}{F_x} = \frac{1}{Eb}\left[\frac{2(2R+t)}{\sqrt{t(4R+t)}}\left(\arctan\sqrt{1+\frac{4R}{t}} - \frac{\pi}{2}\right)\right] \quad (A.11)$$

Shear compliance: shear modulus, $G = E/[2(1+\nu)]$, α is shear correction factor

$$\left[\frac{\Delta y}{F_y}\right]_s = \frac{\alpha E}{G}\frac{\Delta x}{F_x} \quad (A.12)$$

A.3. Wu and Zhou [10]

$$s = R/t$$

$$\frac{\alpha_z}{M_z} = \frac{12}{EbR^2}\left[\frac{2s^3(6s^2+4s+1)}{(2s+1)(4s+1)^2} + \frac{12s^4(2s+1)}{(4s+1)^{5/2}}\arctan\sqrt{4s+1}\right] \quad (A.13)$$

$$\frac{\Delta y}{F_y} = \frac{12}{Eb}\left[\frac{s(24s^4+24s^3+22s^2+8s+1)}{2(2s+1)(4s+1)^2} + \frac{(2s+1)(24s^4+8s^3-14s^2-8s-1)}{2(4s+1)^{5/2}} \times \left(\arctan\sqrt{4s+1}+\frac{\pi}{8}\right)\right] \quad (A.14)$$

$$\frac{\Delta x}{F_x} = \frac{1}{Eb}\left[\frac{2(2s+1)}{\sqrt{4s+1}}\arctan\sqrt{4s+1} - \frac{\pi}{2}\right] \quad (A.15)$$

Shear compliance: shear modulus, $G = E/[2(1+\nu)]$

$$\left[\frac{\Delta y}{F_y}\right]_s = \frac{1}{Gb}\left[\frac{2(2s+1)}{\sqrt{4s+1}}\arctan\sqrt{4s+1} - \frac{\pi}{2}\right] \quad (A.16)$$

A.4. Tseytlin [8]

For thin circular hinges, $t/R \leq 0.07$

$$\frac{\alpha_z}{M_z} = 4\left\{1+\left[1+0.1986\left(\frac{2R}{t}\right)\right]^{1/2}\right\} / \left[Eb\left(\frac{t}{2}\right)^2\right] \quad (A.17)$$

The coefficient 0.1984 may be changed to 0.215 at angle $\theta_m \subseteq \pm 0.9$.

For intermediate circular hinges, $0.07 < t/R \leq 0.2$

$$\frac{\alpha_z}{M_z} = 4\left\{1+\left[1+0.373\left(\frac{2R}{t}\right)\right]^{1/2}\right\} / \left[1.45Eb\left(\frac{t}{2}\right)^2\right] \quad (A.18)$$

For thick circular hinges, $0.2 < t/R \leq 0.6$

$$\frac{\alpha_z}{M_z} = 4\left\{1+\left[1+0.5573\left(\frac{2R}{t}\right)\right]^{1/2}\right\} / \left[2Eb\left(\frac{t}{2}\right)^2\right] \quad (A.19)$$

If Poisson's ration $\nu \neq 0.333$, multiply α_z/M_z by the factor $(1-\nu^2)/0.889$

A.5. Smith et al. [12]

$$I_{zz} = 1/12bt^3$$

$$\frac{\alpha_z}{M_z} = \frac{(1.13t/R+0.332)R}{EI_{zz}} \quad (A.20)$$

A.6. Schotborgh et al. [13]

$$\frac{\alpha_z}{M_z} = \left\{\frac{Ebt^2}{12}\left[-0.0089+1.3556\sqrt{\frac{t}{2R}} - 0.5227\left(\sqrt{\frac{t}{2R}}\right)^2\right]\right\}^{-1} \quad (A.21)$$

References

[1] Paros J, Weisbord L. How to design flexure hinge. Mach Des 1965; 37:151–6.
[2] Handley D, Lu T-F, Yong Y. Workspace investigation of a three DOF compliant micro-motion stage. In: Proceedings of the eighth international conference on control, automation, robotics and vision. 2004. p. 1279–84.
[3] Scire F, Teague E. Piezodriven 50- μ m range stage with subnanometer resolution. Rev Sci Instrum 1978;49(12):1735–40.
[4] Gao P, Swei S, Yuan Z. A new piezodriven precision micropositioning stage utilizing flexure hinges. Nanotechnology 1999;10:394–8.
[5] Her I, Chang J. A linear scheme for the displacement analysis of micropositioning stages with flexure hinges. J Mech Des 1994;116:770–6.
[6] Jouaneh M, Ge P. Modelling and control of a micro-positioning tower. Mechatronics 1997;7(5):465–78.
[7] Yi B-J, Chung G, Na H, Kim W, Suh I. Design and experiment of a three-DOF parallel micromechanism utilizing flexure hinges. IEEE Trans Robot Auto 2003;19(4):604–12.
[8] Tseytlin Y. Notch flexure hinges: an effective theory. Rev Sci Instrum 2002;73(9):3363–8.
[9] Lobontiu N, Paine J, Garcia E, Goldfarb M. Corner-filleted flexure hinges. J Mech Des 2001;123:346–52.
[10] Wu Y, Zhou Z. Design calculations for flexure hinges. Rev Sci Instrum 2002;73(9):3101–6.
[11] Lobontiu N. Compliant mechanisms: design of flexure hinges. CRC Press; 2003.
[12] Smith S, Chetwynd D, Bowen D. Design and assessment of monolithic high precision translation mechanisms. J Phys E 1987;20:977–83.
[13] Schotborgh W, Kokkeler F, Trager H, van Houten F. Dimensionless design graphs for flexure elements and a comparison between three flexure elements. Precis Eng 2005;29:41–7.
[14] Smith S, Badami V, Dale J, Xu Y. Elliptical flexure hinges. Rev Sci Instrum 1997;68(3):1474–83.
[15] Lobontiu N, Paine J, Garcia E, Goldfarb M. Design of symmetric conic-section flexure hinges based on closed-form compliance equations. Mech Mach Theory 2002;37:477–98.
[16] ANSYS. ANSYS element reference. ANSYS Inc.; 2002.
[17] Lobontiu N, Paine J, O'Malley E, Samuelson M. Parabolic and hyperbolic flexure hinges: flexibility, motion precision and stress characterization based on compliance closed-form equations. Precis Eng 2002;26:183–92.